Computational Study of Proton Transfer in Tautomers of 3- and 5-Hydroxypyrazole Assisted by Water

ARTICLE *in* CHEMPHYSCHEM · JUNE 2015

Impact Factor: 3.42 · DOI: 10.1002/cphc.201500317

4 AUTHORS:

Cristina Trujillo
Trinity College Dublin
36 PUBLICATIONS **392** CITATIONS
SEE PROFILE

Goar Sánchez
University College Dublin
69 PUBLICATIONS **900** CITATIONS
SEE PROFILE

Ibon Alkorta
Spanish National Research Council
679 PUBLICATIONS **12,401** CITATIONS
SEE PROFILE

José Elguero
Spanish National Research Council
1,502 PUBLICATIONS **22,187** CITATIONS
SEE PROFILE

ChemPubSoc Europe
DOI: 10.1002/cphc.201500317
CHEMPHYSCHEM Articles

Computational Study of Proton Transfer in Tautomers of 3- and 5-Hydroxypyrazole Assisted by Water

Cristina Trujillo,*[a] Goar Sánchez-Sanz,[b] Ibon Alkorta,[c] and José Elguero[c]

The tautomerism of 3- and 5-hydroxypyrazole is studied at the B3LYP, CCSD and G3B3 computational levels, including the gas phase, PCM–water effects, and proton transfer assisted by water molecules. To understand the propensity of tautomerization, hydrogen-bond acidity and basicity of neutral species is approached by means of correlations between donor/acceptor ability and H-bond interaction energies. Tautomerism processes are highly dependent on the solvent environment, and a significant reduction of the transition barriers upon solvation is seen. In addition, the inclusion of a single water molecule to assist proton transfer decreases the barriers between tautomers. Although the second water molecule further reduces those barriers, its effect is less appreciable than the first one. Neutral species present more stable minima than anionic and cationic species, but relatively similar transition barriers to anionic tautomers.

1. Introduction

The study of tautomerism is fundamental to understand the overall physical and biological properties of a molecule. As tautomers are different compounds (in the solid state they are desmotropes not polymorphs),[1] their physical properties differ, for instance, host–guest abilities,[2] UV,[3] IR,[4] photophysics,[5] proton conduction,[6] molecular electronics,[7,8] and many more.

Tautomers are also important in biological sciences, because the interaction between small molecules (drugs, metabolites, hormones, and ligands in general) and receptors is mediated by noncovalent interactions such as hydrogen bonds (HB), π stacking, dispersion forces, and so forth. Examples have been discussed in the general field of genetics,[9] and more specifically in mutagenesis,[10] receptor ligands,[11] enzyme catalysis,[12] the tautomerism of histidine,[13,14] and so forth. Proton conduction is also relevant in biological molecules.[15]

All these properties are related to the tautomeric structure, but not in a simple way. According to the Winstein–Holness equation,[16–18] reactivity can be expressed as the product of two terms; one corresponding to the amount of each species in the equilibrium mixture, that is, their relative stability, and the other to the intrinsic reaction rate of each species. In addition, the Gustafsson paradox[19–23] states that the less abundant tautomer is the most reactive. Thus, it is difficult to predict the reactivity of tautomerizable compounds, as the two terms tend to counteract each other.

Scheme 1 can be used to simulate drug–receptor interactions of pyrazolinone (where AH and HA represent two tautomers). The affinity for the receptor can be approximated using hydrogen-bonded complexes. The Gustafsson paradox corresponds, for instance, to AH being more stable than HA, but HA forming stronger HBs with R than AH.

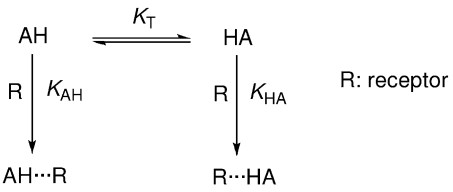

Scheme 1.

The compounds studied in this work are represented in Figure 1; these include compounds belonging to the hydroxypyrazole family (**1a**, *Z*; **1b**, *E*; **4a**, *Z*; **4b**, *E*) and pyrazolinones **2** and **3**. Highly unstable tautomers, such as those having N=N bonds or two C=N bonds, were not considered.[21,24,25]

A good knowledge of the equilibria involved is necessary, not only for the neutral species, but also for the charged ones (protonated and deprotonated), as the reactivity is often catalyzed by Lewis and Brønsted acids and bases (Figure 2). If the tautomerizable proton is removed, several neutral tautomers can result in the same anionic tautomer.

For this study we have selected pyrazolinones (3-hydroxypyrazoles) for the following reasons and restraints:

1. They are much-studied compounds, both experimentally and theoretically.

[a] Dr. C. Trujillo
School of Chemistry, Trinity Biomedical Sciences Institute
Trinity College Dublin, 152-160 Pearse St.
Dublin 2 (Ireland)
E-mail: trujillc@tcd.ie
[b] Dr. G. Sánchez-Sanz
School of Physics & Complex and Adaptive Systems Laboratory
University College Dublin, Belfield, Dublin 4 (Ireland)
[c] Prof. I. Alkorta, Prof. J. Elguero
Instituto de Química Médica, CSIC
Juan de la Cierva, 3, 28006 Madrid (Spain)

Supporting Information for this article is available on the WWW under http://dx.doi.org/10.1002/cphc.201500317.

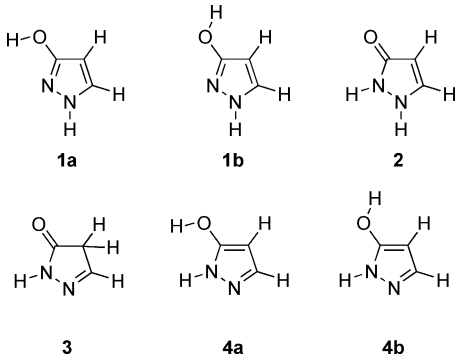

Figure 1. Tautomers and conformers of 3- and 5-hydroxy-1*H*-pyrazole: 3-hydroxy-1*H*-pyrazole (**1a** and **1b**), 1*H*-3-pyrazolin-5-one (**2**), 1*H*-2-pyrazolin-5-one (**3**), and 5-hydroxy-1*H*-pyrazole (**4a** and **4b**).

2. Many drugs contain the pyrazolinone skeleton, some of them are represented in Figure 3. In fact, a recent study has stressed the importance of the hydroxylaminopyrazolone (HAPY) class of HNO donors in vasorelaxation and myocardial contractility.[26] The drugs shown in Figure 3 were selected from two consecutive reviews on drug-related pyrazoles.[27,28]
3. For the present work, we decided to study the simplest compound, pyrazolinone itself (3- and 5-hydroxy-1*H*-pyrazole), which can exist as four main tautomers and five structures (**a** and **b** corresponds to the two positions of the OH group of the same tautomer; Figure 1).
4. Several previous computational studies have been carried out, which we have summarized in Table 1 and developed in Table 2 for the parent compound.

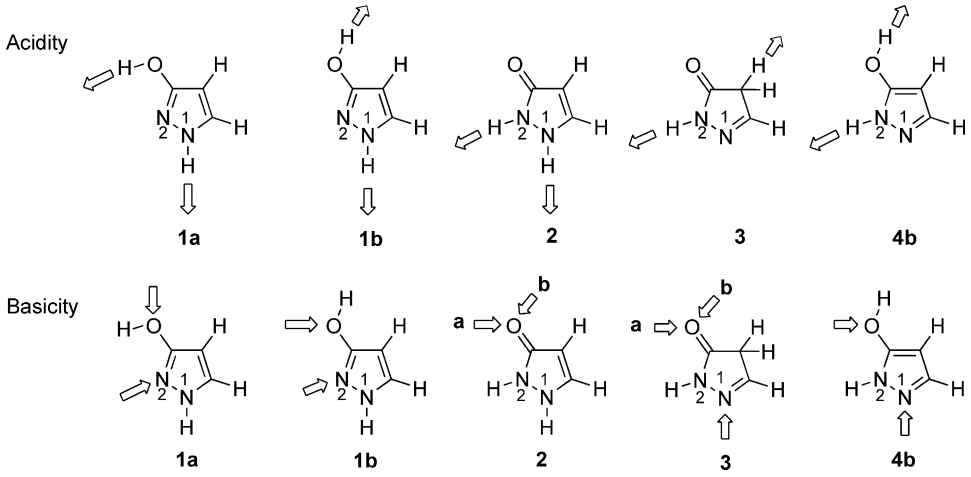

Figure 2. Basicity (proton-gain) and acidity (proton-loss) sites.

Table 1. Previous theoretical studies related to the tautomerism of pyrazolinones in chronological order.

Pyrazolinone	Method	Ref.
4-phenylazo[a]	HMO	[29]
parent	MNDO+CI	[24]
parent	MP4(SDTQ)/6-31G(d,p)/3-21G[b]	[30]
parent	Best estimate[c]	[31]
parent	MP4(SDTQ)/6-311+G(d,p)	[32]
1-methyl	6-31+G(d)/PM3	[33]
1-phenyl-3-methyl	B3LYP/6-31G(d)[b]	[34]
3-CO_2Et	B3LYP/6-31G(d,p)	[35]
1-dinitrophenyl-3-methyl	B3LYP/6-31G(d)	[36]
parent	MP2/6-31G(d,p)	[37]
3-methyl	6-31G(2p,d)	[38]
1-phenyl-3-methyl	B3LYP/6-31+G(d)	[39]
1-phenyl-3-methyl-4-*R*	MP2/6-31G(d,p) and B3LYP/6-311G(d,p)	[40]
1-phenyl-4-benzoyloxime[a]	B3LYP/6-31G(d,p)	[41]
1-phenyl-3-methyl-4-*R*	B3LYP/6-311G(d)	[42]
3-methyl-4-oxime[a]	MP4/6-31+G(d,p)	[43]
1-phenyl-3-methyl	B3LYp/cc-pVDZ[d]	[44]
not reported	MP2/CBS+[CCSD-MP2/6-31+G(d)][e]	[45]
parent	B3LYP/6-31G(d)	[46]
1-phenyl-3-methyl	B3LYP/6-311+G(d,p)	[47]
4-CO_2R	B3LYP/6-311++G(d,p)[d]	[48]

[a] These groups are tautomerizable and intervene in the whole process. [b] Solvent effects (PCM). [c] Solvent effects (SCRF). [d] Solvent effects (IEF–PCM). [e] Solvent effects (IEF–MST).

Some of these data have been reported in books and in book chapters.[21,25,49,50]

The most reliable results are those of Refs. [31, 32 and 37], which we have averaged in the last column of Table 2.[47,48]

Computational Details

The geometry of the monomers and the complexes were fully optimized using density functional theory (DFT) methods, at the B3LYP[51,52] level with the standard 6-311++G(d,p)[53] basis set. Harmonic vibrational frequencies were computed at the same level used for the geometry optimizations to classify the stationary points either as local minima or transition states (TS). All of these calculations were carried out with the Gaussian09 program.[54] Final energies were calculated using CCSD and CCSD(T) single-point calculations over the B3LYP/6-311++G(d,p) optimized geometry combined with the aug-cc-pVTZ[55,56] basis set. To assess the reliability of this scheme we also obtained the final energies, as well as optimized structures of the different stationary points, using G3B3[57] theory. This theoretical scheme has been proven to be accurate for a large set of molecules.[57] Hydration effects were analyzed for the tautomers and for the transition states connecting them by using the following mixed model. Specific hydration effects were taken into account by considering hydrated complexes

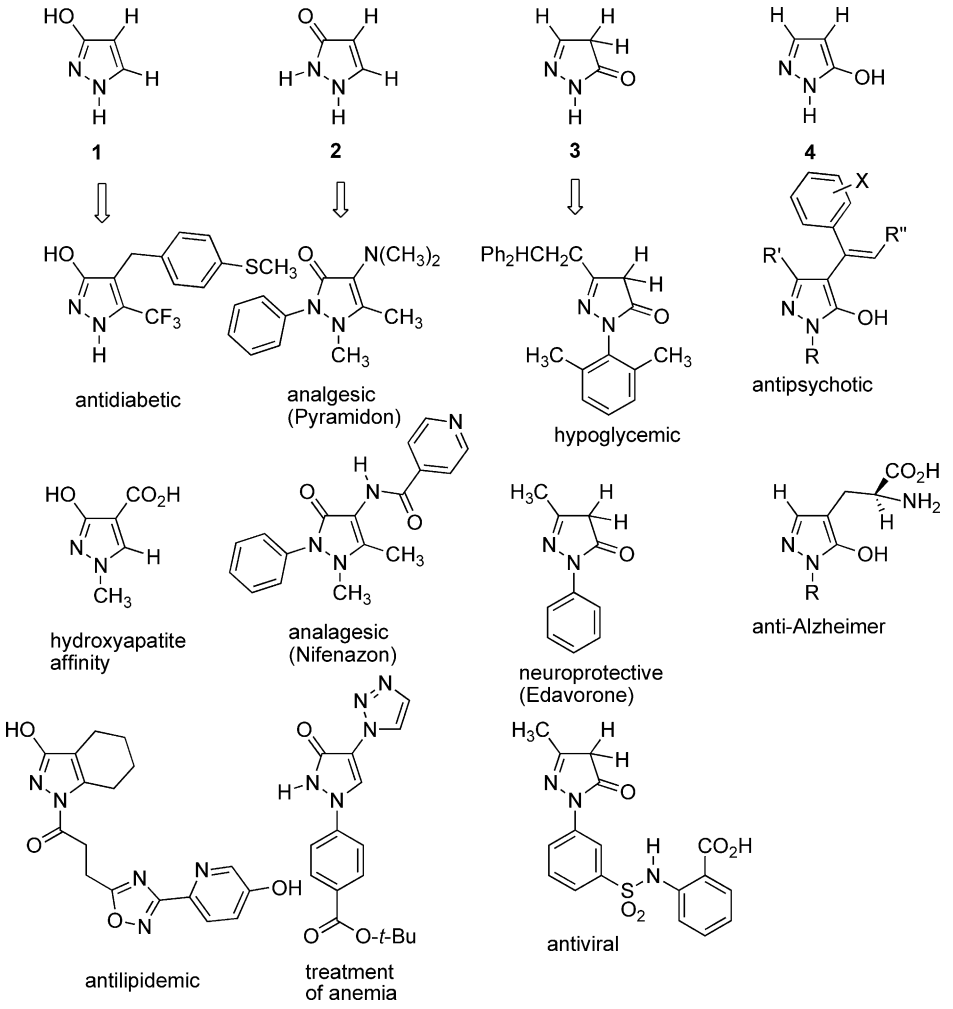

Figure 3. Some examples of drugs with pyrazole-type skeletons.

Table 2. Relative energies [kJ mol^{-1}] of the different tautomers of Figure 1.

Tautomer	Ref. [24] Gas phase	[30] Gas phase	[30] Water	[30,31] Gas phase	[32] Gas phase	[37] Gas phase	[46] Gas phase	Average Gas phase
1a	0.0	9.9	14.7	0.0	0.0	0.0	57.7	0.0
1b	—	—	—	13.8	11.7	—	—	12.8 ± 1.0
2	56.9	0.0	0.0	31.4	23.8	42.8	0.0	32.7 ± 10
3	16.4	37.6	28.4	9.6	—	4.6	13.4	7.1 ± 2.5
4b	4.9	24.7	28.7	17.2	—	14.5	—	15.8 ± 1.4

with one and two molecules of water. The effect of the bulk was then accounted for by using SCFR–PCM[58] approaches implemented in the Gaussian09 package and dispersing, repulsing, and cavitation energy terms of the solvent were included in the optimization.

Bonding characteristics were analyzed by means of the atoms in molecules (AIM) theory.[59] For this purpose we located the most relevant bond critical points (BCP), and evaluated the electron density at each of these points, with the help of the AIMAll program.[60]

2. Results and Discussion

2.1. Neutral Compounds

2.1.1. Tautomer Stability

The neutral compounds studied are summarized in Figure 4. Minima are labeled with numbers, plus "**a**" or "**b**" for those with an hydroxy group to differentiate whether the hydrogen atom of the hydroxy groups is oriented towards the nitrogen atoms (**a**) or towards the carbon atoms (**b**). In addition, each transition state between the minima is labeled with the prefix TS and numbers indicating the minima to which it is connected. For example, **TS$_{rot}$ 1a_1b** represents the transition state corresponding to rotation of the hydroxy group connecting the **1a** and **1b** minima. Notably, tautomer **4a** isomerizes spontaneously into **4b**, therefore from here on only **4b** will be taken into account in the discussion.

In addition, to consider all possible tautomers, structures **5**–**7** were optimized at the G3B3 computational level both in the gas phase and in PCM–water (Figure 5). Their relative energies with respect to tautomer **1a** in PCM–water are 75.8, 164.6, and 178.7 kJ mol^{-1} respectively. They lie at high energy, and therefore, they were not be included in the potential energy surfaces and are not considered in the rest of this manuscript.

The relative energies with respect to the most stable tautomer are shown in Table 3. Energies from B3LYP/6-311++G(d,p) gas-phase calculations show that the most stable compound is **1a**. Compounds **1b**, **2**, and **4b**, lie at 15.2, 18.9, and 16.8 kJ mol^{-1} with respect to **1a**, whereas **3** is only 3.2 kJ mol^{-1} higher than **1a**. CCSD and CCSD(T) gas-phase calculations gave slightly different results. **1b** lies at 13.3 and 13.1 kJ mol^{-1}, respectively, almost 2 kJ mol^{-1} lower than the values obtained through DFT calculations. **2** is more unstable, showing a relative energy of 29.4 kJ mol^{-1} [30.6 in CCSD(T)]. Tautomer **3** slightly increases its relative energy from 3.2 kJ mol^{-1} in B3LYP, up to 6.0 kJ mol^{-1} in CCSD and slightly larger (8.6 kJ mol^{-1}) in CCSD(T). Finally, the relative energy of **4b** is almost constant across all tested methods. Notably, CCSD and CCSD(T) provide almost the same results. Additionally, the computational cost of CCSD(T) is much higher than that of CCSD. Thus, as CCSD

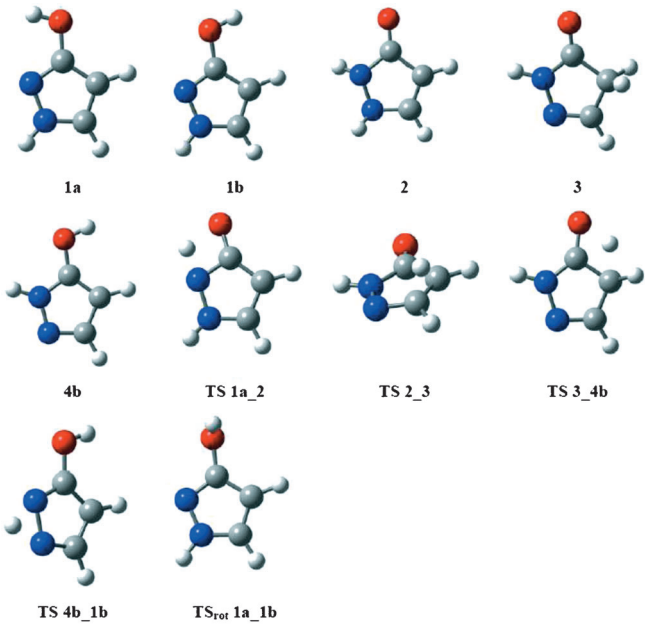

Figure 4. Optimized structures, minima, and transition states for tautomers studied at the B3LYP/6–311++G(d,p) computational level.

Figure 5. Optimized structures for tautomers **5**, **6**, and **7** at the G3B3 computational level.

Table 3. Relative energies (ΔE) with respect to the most stable tautomer (**1a**; shown in bold) at B3LYP/6–311++G(d,p), CCSD(T), CCSD/aug-cc-pVTZ, and G3B3 computational levels in the gas phase and in PCM–water.

	Gas phase				PCM–water			
	B3LYP	CCSD	CCSD(T)	G3B3	B3LYP	CCSD	CCSD(T)	G3B3
1a	**0.0**	**0.0**	**0.0**	**0.0**	**0.0**	**0.0**	**0.0**	**0.0**
1b	15.2	13.3	13.1	12.9	3.9	3.3	3.3	3.5
2	18.9	29.4	30.6	31.6	1.8	15.2	16.2	17.2
3	3.2	6.0	8.6	6.4	-1.6	0.7	3.9	2.6
4b	16.8	16.4	16.7	16.4	12.7	12.8	13.0	12.6
TS 1a_2	221.0	240.3	226.9	214.1	213.7	232.3	219.5	206.5
TS 2_3	217.5	246.2	226.4	216.7	197.9	224.9	207.7	199.3
TS 3_4b	298.0	314.0	301.0	286.3	297.8	313.8	301.1	286.4
TS 4b_1b	225.2	228.2	216.7	205.5	219.1	223.1	212.0	201.4
TS$_{rot}$ 1a_1b	20.8	18.7	18.6	16.8	13.1	12.0	12.0	10.3

has been verified to be a good approach and is computationally more affordable than CCSD(T), the latter will not be considered further.

When we compared our results with the best literature results (Table 2; best estimate[31] and average), we found the following regression lines [Eqs. (1)–(3)]:

$$\text{CCSD} = (0.98 \pm 0.03)\ \text{G3B3},\ n = 5,\ R^2 = 0.996 \quad (1)$$

$$\text{Average} = (0.99 \pm 0.04)\ \text{best estimate},\ n = 5,\ R^2 = 0.993 \quad (2)$$

$$\text{CCSD} = (1.06 \pm 0.13)\ \text{best estimate},\ n = 5,\ R^2 = 0.940 \quad (3)$$

Equations (1) and (2) show the internal consistencies between the literature and the present work, whereas Equation (3), which is the slightly worse in terms of thecorrelation coefficient, corresponds to the comparison of our calculations with those in the literature. The differences are too subtle to be discerned by experimental results,[25] and mainly concern the less stable tautomers, which are not observed experimentally owing to their low populations.

The rotation barrier (**TS$_{rot}$ 1a_1b**) that connects **1a** and **1b**, lies between 18.6 and 20.8 kJ mol^{-1}, from B3LYP, CCSD, and CCSD(T) levels in the gas phase, over the entrance channel, and is relatively low compared with the other transition states. The rest of the transition states are much higher, as their relative energy ranges between 216.7 and 314.0 kJ mol^{-1}, for B3LYP, CCSD, and CCSD(T) calculations in the gas phase. If we take into account G3B3 gas-phase results, the relative energies of the minima resemble those found by CCSD and CCSD(T) calculations, however, transition barriers are substantially lower (see Table 3).

With regards to the effect of solvation on the relative energy, the inclusion of solvent (PCM–water) decreases the relative energies at the B3LYP, CCSD, CCSD(T), and G3B3 computational levels. Those minima with the largest dipole moments, **1b** and **2** (3.6 and 5.2 D), present the largest variations in their relative energies upon inclusion of the PCM–water model. The G3B3 method provides the smallest transition barriers. As both B3LYP and G3B3 provide similar structures and the relative energies corresponding to the minima at G3B3, CCSD, and CCSD(T) methods are close, only G3B3 structures will be considered for the potential energy surface diagrams in neutral molecules, anions, and cations, whereas the other methods will be taken into account only in the neutral molecules for comparison purposes.

2.1.2. Hydration Effects

The energy profiles of tautomerism for the corresponding mono- and dihydrated species are presented in Figures 6 and 7, respectively. For each tautomerization pathway, relative energies were calculated with respect to the most stable minimum (**1a**). The relative energies of the mono- and dihydrated clusters are given in Table 4.

The energy profile presented in Figure 6 shows that the most important difference between the prototropic tautomerism of monohydrated species and the isolated compound is associated with the activation barriers, which become almost half or even less than half of those obtained for the isolated compound; this is a well-known phenomenon.[61–68] Considering the G3B3 gas-phase data, the inclusion of a molecule of water lowers the barrier between **1a** and **2** from 214.1 to 75.1 kJ mol^{-1}. When the effect of the bulk is added by

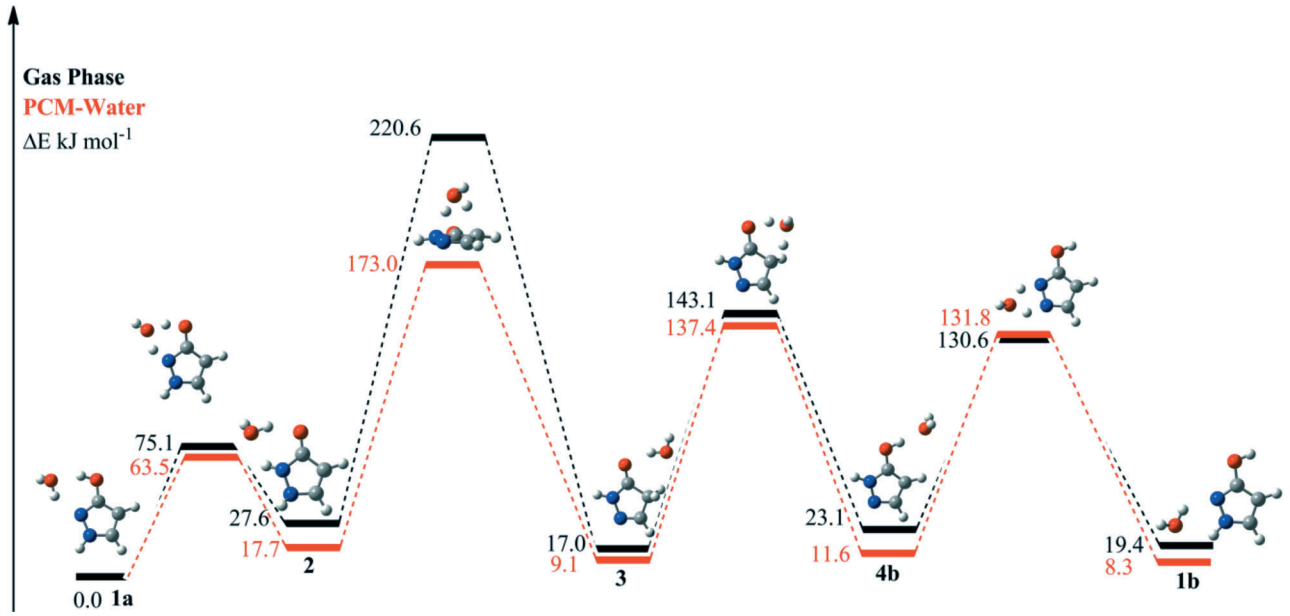

Figure 6. Energy profile for the proton-transfer process assisted by one water molecule, with and without PCM–water. Energies are in kJ mol^{-1} at the G3B3 computational level.

Table 4. Relative energies (ΔE) with respect to the most stable tautomer (**1a**; shown in bold) at B3LYP/6-311++G(d,p), CCSD/aug-cc-pVTZ and G3B3 computational level in gas phase and in PCM-Water with one and two molecules of water.

	Gas Phase			PCM-Water		
	B3LYP	CCSD	G3B3	B3LYP	CCSD	G3B3
H_2O						
1a	**0.0**	**0.0**	**0.0**	**0.0**	**0.0**	**0.0**
1b	22.7	18.6	19.4	9.9	10.0	8.3
2	17.1	27.0	27.6	5.9	17.4	17.7
3	16.4	14.6	17.0	8.0	9.4	9.1
4b	23.7	24.4	23.1	11.0	12.7	11.6
TS 1a_2	83.0	103.2	75.1	72.8	91.2	63.5
TS 2_3	236.2	248.3	220.6	182.3	188.5	173.0
TS 3_4b	153.9	172.6	143.1	146.8	162.8	137.4
TS 4b_1b	146.0	160.2	130.6	148.2	159.2	131.8
$2H_2O$						
1a	**0.0**	**0.0**	**0.0**	**0.0**	**0.0**	**0.0**
1b	15.1	11.7	13.7	14.6	11.5	13.0
2	11.1	21.9	23.0	5.6	16.9	17.6
3	23.7	21.4	25.9	23.1	20.3	25.2
4b	29.7	24.9	25.6	24.1	25.0	25.9
TS 1a_2	69.0	94.1	58.4	62.9	84.8	49.3
TS 2_3	170.9	290.3	156.5	137.1	149.6	126.5
TS 3_4b	132.4	153.8	119.5	118.0	134.5	108.6
TS 4b_1b	102.5	120.9	84.3	94.3	110.5	81.8

enclosing this monohydrated species in a solvent cavity, the changes observed in the energy profile are small (see Figure 6), except for **TS 2_3**, for which the barrier decreases from 199.3 to 173.0 kJ mol^{-1}.

When a second water molecule was added to the complex, as shown in Figure 7, some significant changes in the energetic profile of the prototropic tautomerism were found. Notably, the activation barrier values decrease in almost all cases. Taking into account PCM energy values, the energy barriers corresponding to **TS 3_4b** and **TS 4b_1** decrease by 46.9 and 44.9 kJ mol^{-1} respectively. The most significant change occurs to **TS 2_3**, for which the barrier decreases by 60.0 kJ mol^{-1}.

2.2. Calculation of HB Basicity and Acidity

To assess the HB basicity (HBB) and acidity (HBA) of the neutral compounds, we followed the procedure described by Platts,[69,70] in which the HBB and HBA are related to the different properties that arise from the interactions between the studied compound and a hydrogen donor and acceptor.

Herein, we have approached this problem by using hydrogen fluoride (HF) as the hydrogen donor to obtain HBB (β) and hydrogen cyanide (HCN) as the hydrogen acceptor to calculate HBA (α). Following the best results found by Platts, we assessed the HBB and HBA by using the interaction energies of the complexes formed with HF and HCN, and their corresponding formulae.[69,70]

2.2.1. Interaction Energies

We calculated the molecular electrostatic potential (MEP) of the minima (**1a**, **1b**, **2**, **3** and **4b**) to locate the areas susceptible to electrophilic and nucleophilic attack. The MEP values obtained for these molecules were plotted on a 0.001 au electron density isodensity surface, which resembles the van der Waals surface (Figure 8). These MEP maps provide an indication of the relative propensity of different sites to interact with HF and HCN molecules.

The interaction energies resulting from the complexation between hydrogen fluoride and hydrogen cyanide and the pyrazolinones are summarized in Table 5. In accordance with Platts' work, the uncorrected interaction energies were selected, as

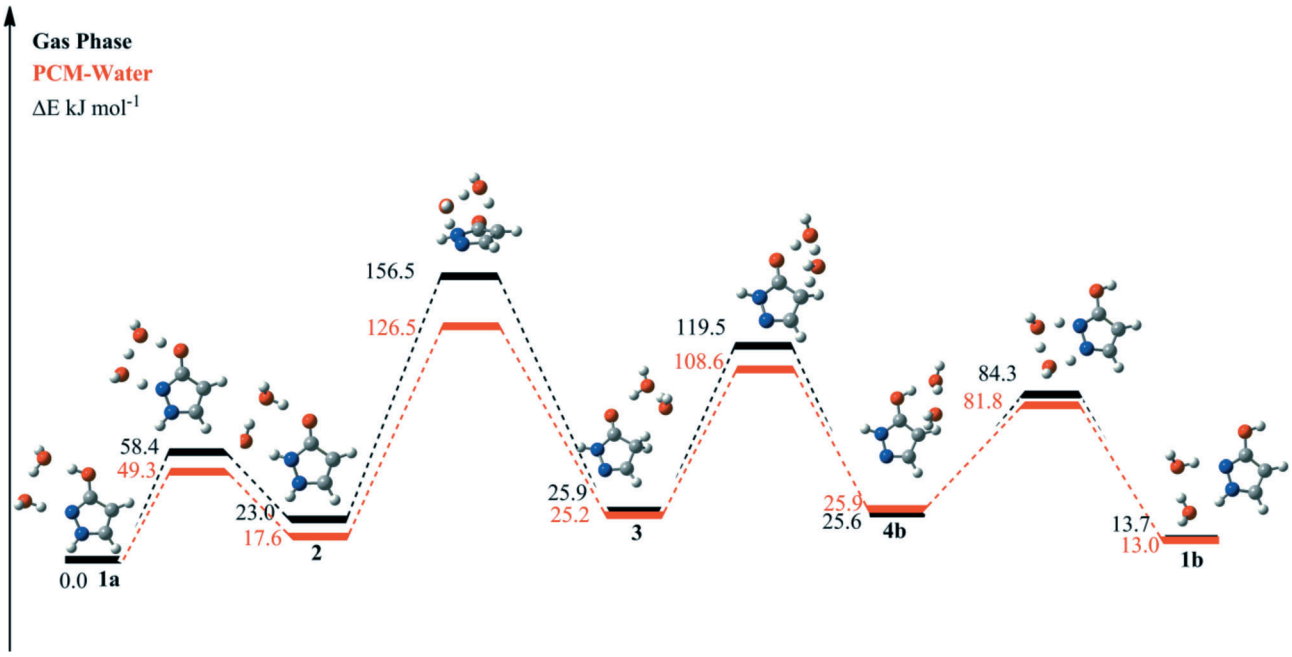

Figure 7. Energy profile for the proton-transfer process assisted by two water molecules, with and without PCM–water. Energies are in kJ mol^{-1} at the G3B3 computational level.

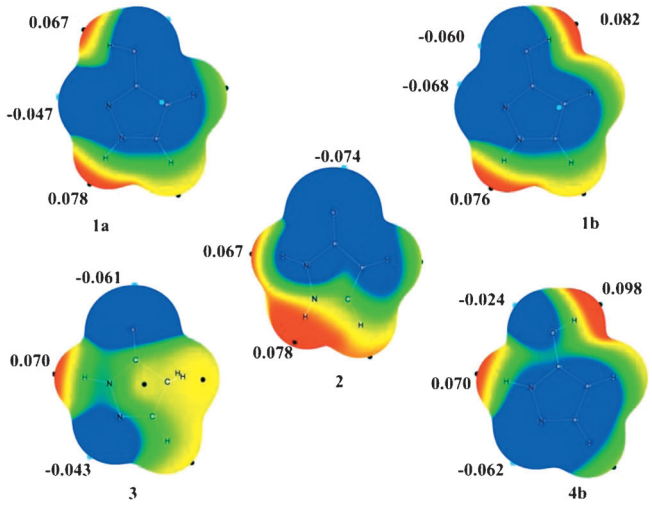

Figure 8. MEP at the 0.001 au electron-density isosurface obtained at the B3LYP/6-311++G(d,p) computational level. Color scheme: red > 0.05, yellow > 0.02, green > 0.00, blue < 0.00. Maxima and minima values of MEP are represented by black and cyan dots respectively.

they have been shown to provide better fitting and results. In this case, in addition to the regular labeling of the minima, an extra label was used to specify the site of the interaction, for example, O stands for the oxygen atom and N1 and N2 for the two different nitrogen atoms (Figure 2). For HCN complexes in the gas phase, interaction energies (kJ mol^{-1}) range from −15.7 to −26.4, −19.2 to −29.5, and −17.9 to −27.0 for the B3LYP, CCSD, and G3B3 methods, respectively, whereas the PCM-water solvent interaction energies range from −29.9 to −38.4 (B3LYP), −14.5 to −22.6 (CCSD), and −12.4 to −20.5 (G3B3). CCSD and G3B3 methods give smaller interaction energies for complexes in a solvent rather than in the gas phase; however, the opposite is true for B3LYP. Nevertheless, the width of the interaction energy ranges remains almost constant across all methods. For all the applied methodologies, the most stable complex corresponds to **4b**(O) with a HCN···H–O interaction, both in gas phase and solvent.

Table 5. Interaction energies (ΔE) in kJ mol^{-1} of the complexes with hydrogen fluoride and hydrogen cyanide at B3LYP/6-311++G(d,p),CCSD/aug-cc-pVTZ//B3LYP/6–311++G(d,p), and G3B3 computational level in gas phase and in PCM-Water. For structures, see Figure 2.

	Gas phase			PCM–water		
	B3LYP	CCSD	G3B3	B3LYP	CCSD	G3B3
HCN						
1a (NH1)	−18.4	−22.0	−19.6	−30.4	−15.2	−13.1
1a (OH)	−15.7	−19.2	−18.0	−33.5	−18.0	−16.2
1b (NH1)	−18.4	−22.0	−19.8	−30.3	−15.1	−13.4
1b (OH)	−20.9	−24.5	−22.3	−35.5	−20.3	−18.6
2 (NH2)	−19.8	−22.0	−20.6	−31.0	−14.7	−13.7
3 (NH1)	−16.5	−19.9	−17.9	−29.9	−14.5	−12.4
4b (NH2)	−16.2	−20.4	−18.3	−30.4	−15.5	−13.2
4b (OH)	−26.4	−29.5	−27.0	−38.4	−22.6	−20.5
HF						
1a (N2)	−56.2	−52.2	−49.1	−51.0	−44.8	−31.8
1a (O)	−34.5	−32.1	−29.9	−46.1	−27.9	−17.0
1a (N2)	−54.6	−49.7	−44.7	−70.7	−47.5	−44.4
1a (O)	−34.9	−31.5	−26.1	−46.9	−28.5	−22.3
2a (O)	−62.3	−59.6	−57.4	−67.6	−51.2	−42.8
2b (O)	−55.2	−52.7	−49.6	−69.5	−52.9	−43.2
3a (O)	−51.3	−51.8	−47.7	−59.5	−41.8	−29.8
3b (O)	−48.1	−48.3	−44.6	−60.4	−43.1	−31.3
3a (N1)	−42.6	−38.3	−32.3	−60.0	−37.9	−34.4
4b (N1)	−55.8	−50.5	−44.7	−73.3	−49.3	−45.3
4b (O)	−29.3	−28.9	−27.5	−40.1	−22.4	−11.2

For HF complexes, both the interaction energies and the width of the interaction-energy ranges are larger than those found for HCN complexes, which suggests that the pyrazolinones have a strong HB-acceptor capacity. Amongst all the compounds, **2a**(O) has the highest interaction energy in the gas phase. However, when the solvent is taken into account, **4a**(N1) complex is the most stable with the B3LYP and G3B3 methods, and **2b**(O) with CCSD.

2.2.2 HBA and HBB

Once the interaction energies between the pyrazolinones and the fluorine acid and hydrogen cyanide were obtained, the HBA and HBB could be derived by using Equations (4) and (5):

$$\alpha(\Delta E) = -0.217 \pm 0.044 + 0.037 \pm 0.002 \cdot \Delta E^{[69]} \quad (4)$$

$$\beta(\Delta E) = -0.101 \pm 0.029 + 0.011 \pm 0.001 \cdot \Delta E^{[70]} \quad (5)$$

The corresponding $\alpha(\Delta E)$ and $\beta(\Delta E)$ values at the B3LYP/6-311++G(d,p) computational levels are shown in Table 6. Equations (4) and (5) were adjusted from B3LYP/6-311++G(d,p) gas-phase calculations, thus, only B3LYP results were used to obtain α and β values. Our α values are between the minimum [dimethylamine ($\alpha = 0.08$)] and maximum [2,2,2-trichloroacetic acid ($\alpha = 0.95$)] values reported by Platts.[69] The same is true for the β values (Table 6), which are between the minimum [acetylene ($\beta = 0.04$)] and maximum [*t*-butylamine ($\beta = 0.71$)] values obtained by Platts.[70]

The acidity of the pyrrolic N–H should be comparable to the α value of pyrrole (0.41; pyrazole = 0.54), the basicity of the pyridinic N atom should be comparable to the β value of pyridine (0.52), the acidity of the O–H group should be comparable to the α value of phenol (0.60), the basicity of the O–H group should be comparable to the β value of phenol (0.30), and the basicity of the C=O moiety should be comparable to the β value of amides (for formamide $\beta = 0.60$).[69,70]

What we actually observe is:

1) The acidity of N–H is 0.41 (**1a**), 0.41 (**1b**), 0.46 and 0.27 (**2**), 0.34 (**3**), and 0.33 (**4b**) with a mean value of 0.37, which is close to that of pyrrole, but reveals that they are weaker acid than pyrazole. Therefore, the O substituents decrease the acidity of pyrazole.

2) The acidity of O–H is 0.31 (**1a**), 0.50 (**1b**), and 0.71 (**4b**), and is very dependent on the position and even the conformation of the OH group; some comformations being weaker HB acids than phenol and some stronger.

3) The basicity of the N atom is 0.52 (**1a**), 0.50 (**1b**), 0.37 (**3a**), and 0.51 (**4b**). The hydroxypyrazoles (**1a**, **1b**, **4b**) are more basic (0.51 in average) than the pyrazolinones (0.37; **3a**) and similar to pyridine.

4) The basicity of the O atom is: a) for OH, 0.28 (**1a**, **1b**) and 0.22 (**4b**) with a mean 0.26, which is similar to phenol (4-fluorophenol $\beta = 0.23$); and b) for C=O, 0.58 (**2a**), 0.51 (**2b**), 0.46 (**3a**), and 0.43 (**3b**) with a mean of 0.50, which is a little lower than the value for formamide (3-chlorobenzamide $\beta = 0.51$).

Table 6. Hydrogen-bonded acidity (α) and basicity (β) values of all compounds studied at B3LYP/6-311++G(d,p) computational level. For structures, see Scheme 2.

	$\alpha(\Delta E)$		$\beta(\Delta E)$
1a (NH1)	0.41	**1a** (N2)	0.52
1a (OH)	0.31	**1a** (O)	0.28
1b (NH1)	0.41	**1b** (N2)	0.50
1b (OH)	0.50	**1b** (O)	0.28
2 (NH1)	0.46	**2a** (O)	0.58
2 (NH2)	0.27	**2b** (O)	0.51
3 (NH1)	0.34	**3a** (O)	0.46
4b (NH2)	0.33	**3b** (O)	0.43
4b (OH)	0.71	**3a** (N1)	0.37
		4b (N1)	0.51
		4b (O)	0.22

2.3. Acid–Base Equilibria

To complete the study, we investigated the tautomerism processes of the ionic species, both anions and cations, both isolated and assisted by one water molecule. The exhaustive study carried out in Section 2.1, led us to conclude that G3B3 provides the most accurate energy values, therefore, only G3B3 results will be analyzed in this section to obtain optimized geometries together with energies for key intermediates and transition states along the studied pathways.

2.3.1. Anions

According to Figure 2, there are five possible anions (Scheme 2), and four transition states connecting them. The optimized geometries for the anions studied are shown in Figure 9.

For **5**, both isomers resulting from the rotation of the hydroxy groups were considered, but isomer **5b** is always less stable than **5a**, thus, a spontaneous isomerization process takes place. Therefore, for the rest of the energy profiles we will only consider **5a**.

As in the neutral case, it is interesting to study the energy profile corresponding to the tautomerism process for the monohydrated species (Figure 10). To transfer the proton from the O atom to the N2 atom, a barrier of 16.4 kJ mol^{-1} (PCM–water) should be overcome, leading to **6.** This is the smallest barrier found in the whole profile; this is because in this transition state (**TS 5a_6**) the hydrogen atom from the OH group is still bound to the oxygen atom with a distance of 1.029 Å. Notably, despite the transition barriers for the neutral species and the anions being more or less the same, the minima found in both cases reveal that neutral tautomers are more stable than anionic ones. This implies that for the neutral complexes more tautomers will be accessible, from a thermodynamic point of view, than for the anionic ones. As occurred in the neutral case, the assistance of a water molecule reduces the transition barriers significantly, in some cases by more than 100 kJ mol^{-1} (see Table 7). The only exception is for **TS 7_8**, in which proton transfer occurs by jumping over the center of the five-mem-

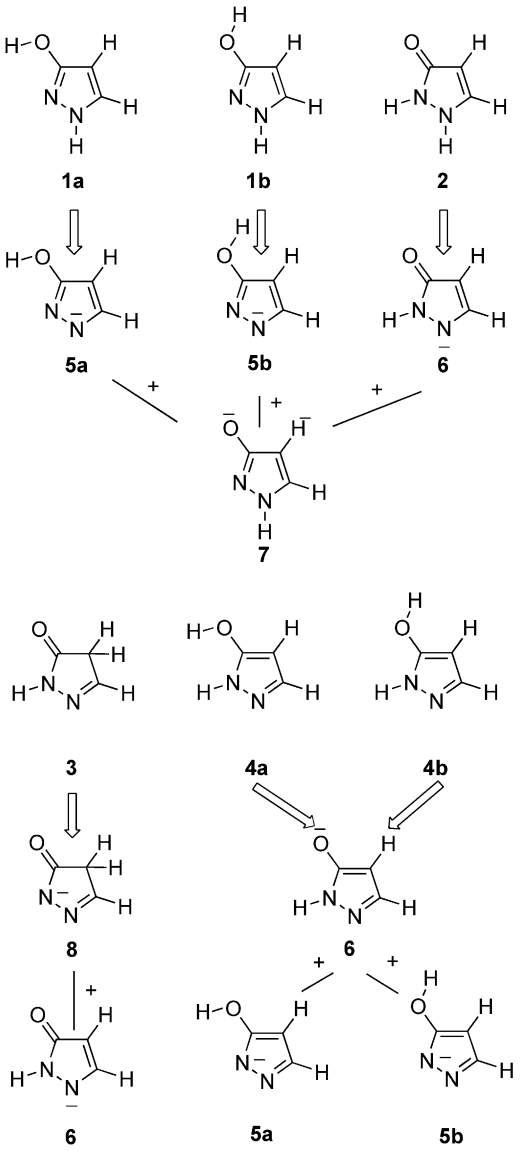

Scheme 2. Origin of the five possible anions, **5**–**8**.

Table 7. Relative energies (ΔE) with respect to the most stable anion (**6**; shown in bold) at the G3B3 computational level in gas phase and in PCM–water, isolated and assisted by one molecule of water.

	Isolated		H_2O	
	Gas phase	PCM–water	Gas phase	PCM–water
5a	37.1	33.9	25.7	28.1
6	**0.0**	**0.0**	**0.0**	**0.0**
7	53.9	18.2	32.7	10.4
8	43.3	30.3	39.5	27.8
TS 5a_6	180.4	193.7	34.9	44.5
TS 6_7	187.6	186.0	104.5	97.9
TS 7_8	220.8	199.8	306.0	231.8
TS 8_5a	276.8	282.5	141.0	146.7

bered ring, and therefore, the assistance of the water molecule slightly increases the energy barrier.

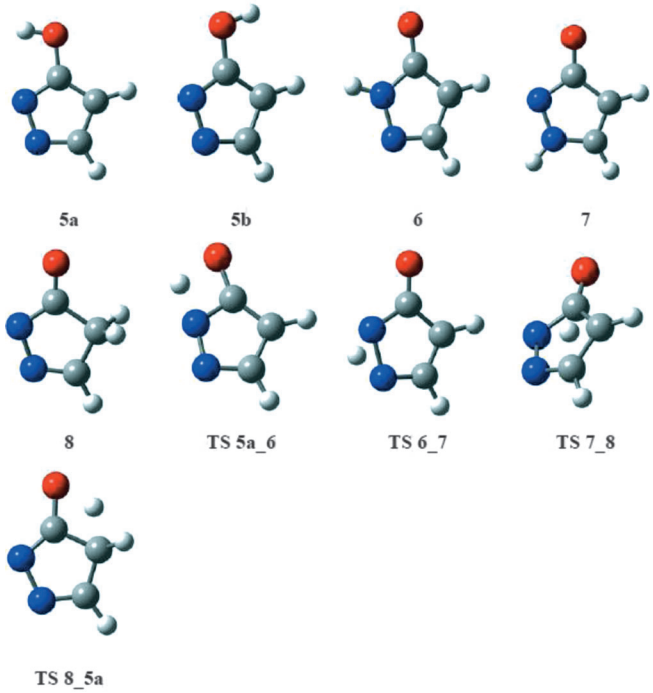

Figure 9. Optimized structures, minima and transition states, for anions studied at G3B3 computational level.

2.3.2. *Cations*

From Figure 2, we generated all the possible tautomers that correspond to protonated neutral structures. However, despite there being eight possible compounds (**9**–**16**), some of them (**11**, **12**) are less likely to be found, because they correspond to nonaromatic structures and the lone pair of N1, which contributes to the aromaticity of **1a**, **1b**, and **2**, is involved in the protonation (Scheme 3). For tautomer **3**, as it is already nonaromatic, cation **14** should be taken into account as well. Cations **10**, **11**, and **15** may present different isomers, **a** or **b**, depending on the position of the hydrogen atom of the OH group (see Scheme 3). As both isomers are close in energy, an isomerization process will occur between them. So, for the sake of clarity, only isomer **a** was taken into account in the energy profiles. However, it is important to highlight that all possibilities were explored, but only the most stable one was taken into account. Specifically, from **10b** we could obtain tautomer **13**, but this path is less stable than the one obtained via **10a** (**TS 10_11**). Figure 11 contains the eight optimized cationic tautomers and the corresponding transition states that connect them.

Notably, protonation of tautomer **2** at the N2 atom gives the cationic tautomer **17**. However, this structure is not stable, probably due to ring tension and loss of aromaticity, and it eventually becomes the ring-opened structure **18** (Figure 12).

As in the previous sections, the tautomeric processes were studied in the presence and absence of a water molecule (Table 8). As is observed in Figure 13, the assistance of one water molecule decreases all energy barriers. Significantly, the relative energies of the minima with respect to the most stable

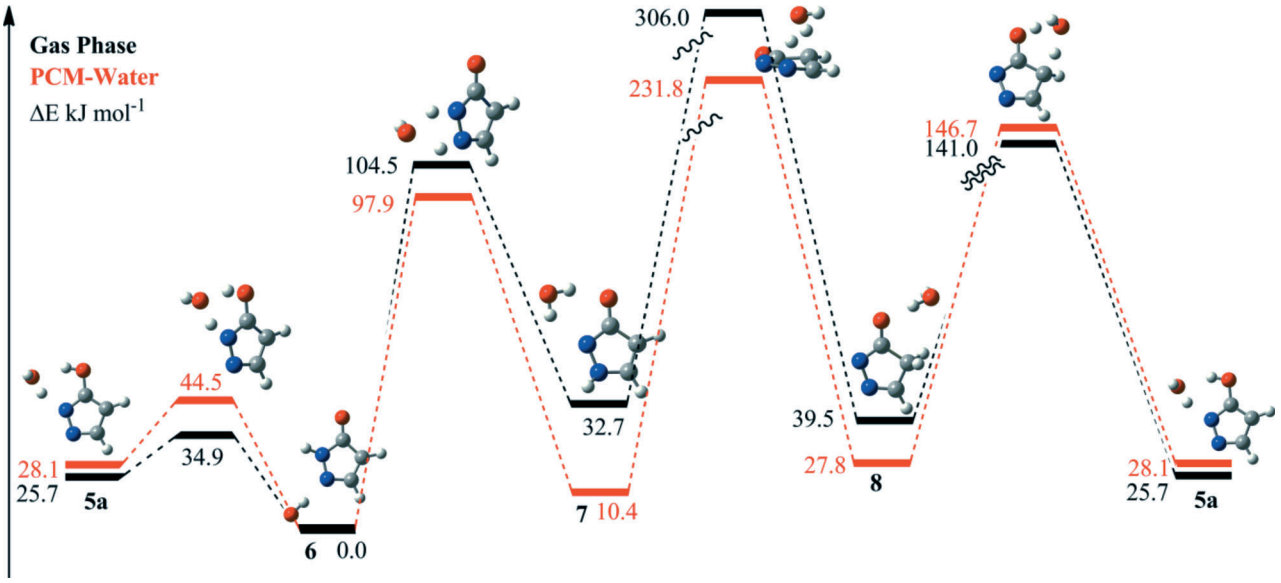

Figure 10. Energy profile for proton-transfer process assisted by one water molecule, with and without PCM–water. Energies are in kJ mol^{-1} at the G3B3 computational level.

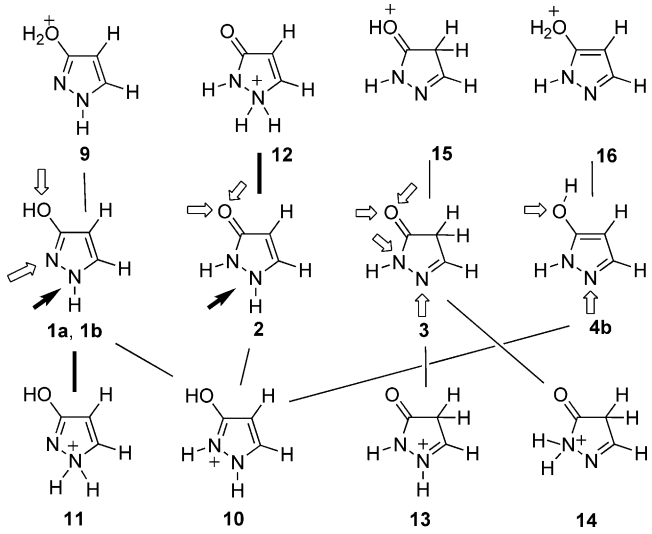

Scheme 3. Origin of the eight possible cations, **9**–**16**.

tautomer are larger in cations than those found in the neutral and anionic ones.

3. Conclusions

As shown by ourselves and others, the inclusion of explicit water molecules is essential to obtain reasonable transition states for proton-transfer mechanisms. This considerably complicates the calculations, but without them, the barriers are highly unrealistic.

A comparative study of three different methods was performed on neutral species to obtain the highest accuracy possible and more reliable structures. Despite the B3LYP method affording good results, CCSD and G3B3 provide a better picture of the energetics, both in the gas phase and in a water solution (PCM–water).

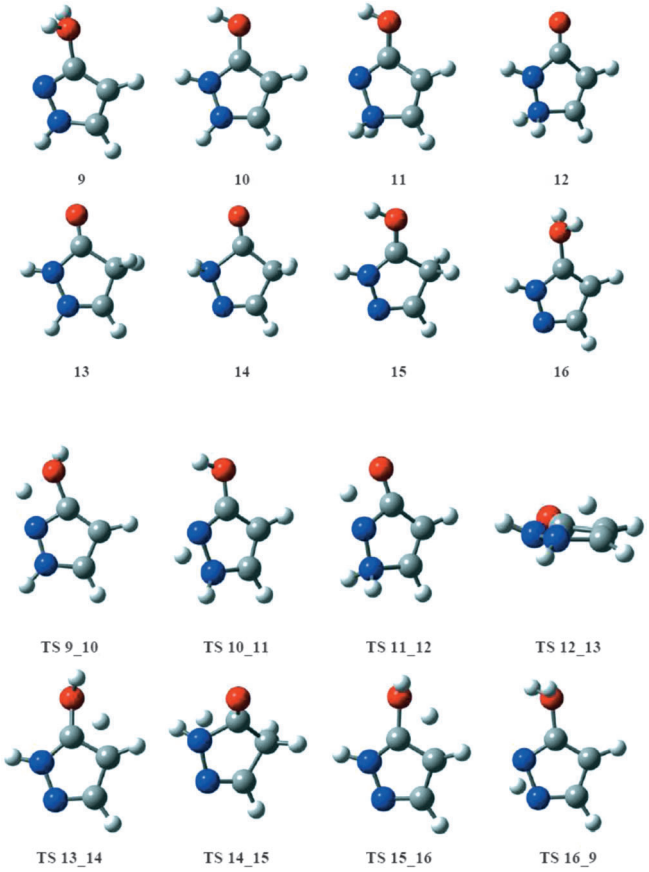

Figure 11. Optimized structures, minima and transition states, for cations studied at G3B3 computational level.

For neutral tautomers, it was shown that the inclusion of PCM–water solvent effects reduces the transition barriers between tautomers. The addition of a single water molecule to assist the proton transfers between tautomers significantly de-

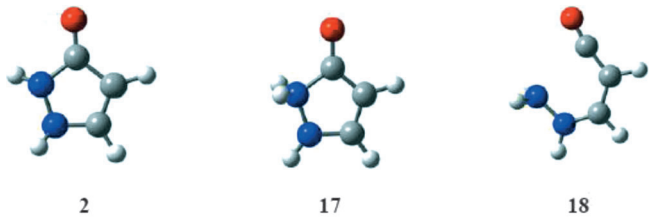

Figure 12. Ring opening by protonation of **2** on N2.

Table 8. Relative energies (ΔE) with respect to the most stable cation (**10**) at G3B3 computational level in gas phase and in PCM–water, isolated and assisted by one molecule of water.

	Isolated		H_2O	
	Gas phase	PCM–water	Gas phase	PCM–water
9	150.1	144.2	177.1	165.0
10	0.0	0.0	0.0	0.0
11	89.5	84.4	102.2	93.7
12	123.4	82.6	120.4	86.5
13	67.3	41.2	63.1	43.7
14	102.5	86.4	101.2	91.7
15	52.9	47.1	39.5	40.3
16	220.9	177.4	165.3	120.5
TS 9_10	233.7	246.1	189.1	188.3
TS 10_11	227.6	222.9	145.0	123.8
TS 11_12	321.4	298.4	173.4	147.4
TS 12_13	336.7	297.5	225.0	152.6
TS 13_14	314.6	303.3	169.2	131.5
TS 14_15	318.6	310.7	155.5	127.8
TS 15_16	374.0	366.3	185.1	141.8
TS 16_9	393.4	367.4	309.2	283.5

creases the barriers. However, although the second water molecule favors tautomeric proton transfer, its effect is less notable than the first one.

HBA and HBB of the neutral tautomers were obtained by using hydrogen cyanide and hydrogen fluoride as the HB acceptor and donor, respectively. The α and β values were obtained using Platts' equations and interaction energies. α values depended on the nature of the acid (N–H/O–H) and were comparable to those of pyrrole and phenol. In turn, β values depended on the nature of the base (=N–/OH/C=O) and were related to pyridine, phenol, and amides.

Neutral and anionic species presented similar values for the transition barriers, but higher energy barriers were obtained for the cationic tautomers. As for neutral compounds, for ionic species, tautomeric processes were kinetically favored by the assistance of water molecules, with decreased energy barriers for all cases.

Acknowledgements

We gratefully acknowledge support from the Ministerio de Economía y Competitividad (Project No. CTQ2012-35513-C02-02) and the Comunidad Autónoma de Madrid (S2013/MIT-2841, Fotocarbon). G.S.-S. thanks the Human Frontier Science Program (Project Reference: LT001022/2013-C) for their support. Thanks are given to the Irish Centre for High-End Computing (ICHEC) and the Trinity Center for High-Performance Computing (TCHPC) for the provision of computational facilities. Aoife Crowe and Dr. Cathy Kelly are acknowledged for their careful reading and help.

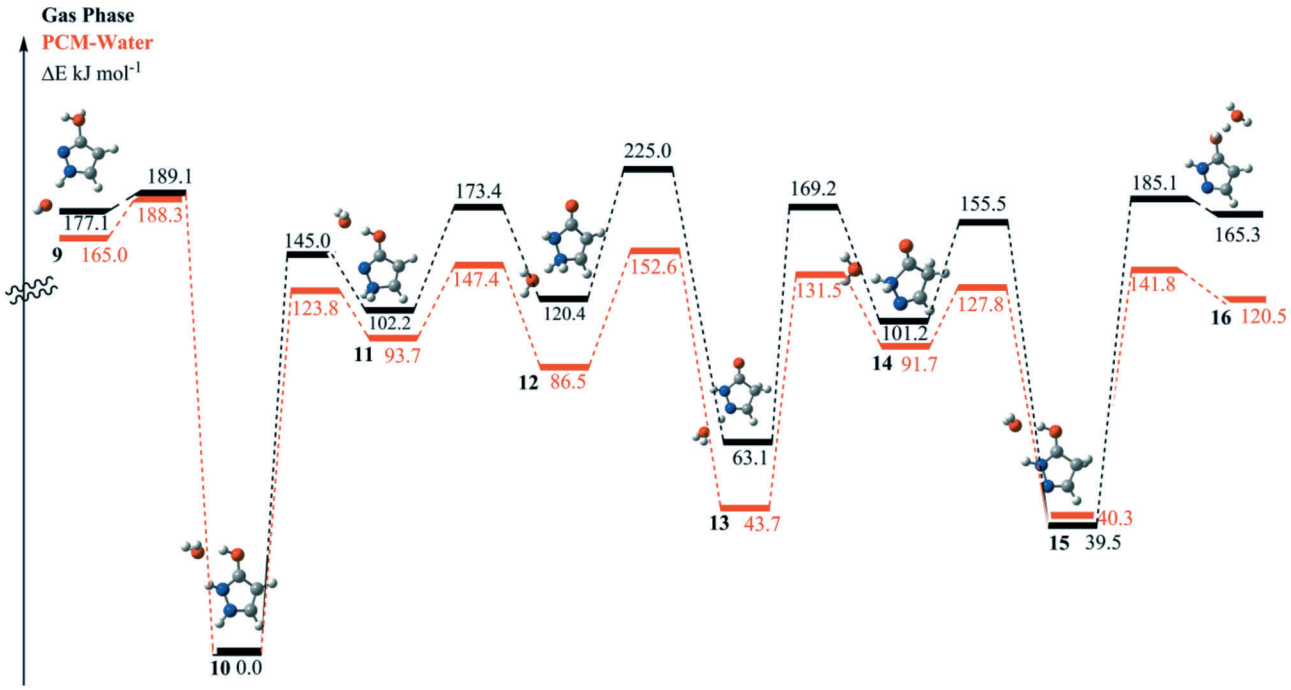

Figure 13. Energy profile for the proton transfer process assisted by one water molecule, with and without PCM-Water. Energies are in kJ mol^{-1} at the G3B3 computational level.

Keywords: computational chemistry · hydration effects · hydroxypyrazole · proton transfer · tautomerism

[1] J. Elguero, *Cryst. Growth Des.* **2011**, *11*, 4731 – 4738.
[2] J. Labuta, Z. Futera, S. Ishihara, H. Kouřilová, Y. Tateyama, K. Ariga, J. P. Hill, *J. Am. Chem. Soc.* **2014**, *136*, 2112 – 2118.
[3] W. Beenken, M. Presselt, T. H. Ngo, W. Dehaen, W. Maes, M. Kruk, *J. Phys. Chem. A* **2014**, *118*, 862 – 871.
[4] P. Touron Touceda, S. Mosquera Vazquez, M. Lima, A. Lapini, P. Foggi, A. Dei, R. Righini, *Phys. Chem. Chem. Phys.* **2012**, *14*, 1038 – 1047.
[5] Z.-H. Pan, J.-W. Zhou, G.-G. Luo, *Phys. Chem. Chem. Phys.* **2014**, *16*, 16290 – 16301.
[6] S. T. Günday, A. Bozkurt, *Polym. J.* **2007**, *40*, 104 – 108.
[7] G. Bussetti, M. Campione, M. Riva, A. Picone, L. Raimondo, L. Ferraro, C. Hogan, M. Palummo, A. Brambilla, M. Finazzi, L. Duò, A. Sassella, F. Ciccacci, *Adv. Funct. Mater.* **2014**, *24*, 958 – 963.
[8] G. J. Simpson, S. W. L. Hogan, M. Caffio, C. J. Adams, H. Früchtl, T. van Mourik, R. Schaub, *Nano Lett.* **2014**, *14*, 634 – 639.
[9] J. Elguero in *Tautomerism, Brenner's Encyclopedia of Genetics, Vol. 7* (Eds.: S. Maloy, K. Hughes), Elsevier-Academic Press, Amsterdam, **2013**, pp. 18 – 22.
[10] B. Kierdaszuk, C. Johansson, T. Drakenberg, R. Stolarski, D. Shugar, *Biophys. Chem.* **1993**, *46*, 207 – 215.
[11] A. B. Reitz, D. A. Gauthier, W. Ho, B. E. Maryanoff, *Tetrahedron* **2000**, *56*, 8809 – 8812.
[12] H. Shimahara, T. Yoshida, Y. Shibata, M. Shimizu, Y. Kyogoku, F. Sakiyama, T. Nakazawa, S.-i. Tate, S.-y. Ohki, T. Kato, H. Moriyama, K.-i. Kishida, Y. Tano, T. Ohkubo, Y. Kobayashi, *J. Biol. Chem.* **2007**, *282*, 9646 – 9656.
[13] J. A. Vila, Y. A. Arnautova, Y. Vorobjev, H. A. Scheraga, *Proc. Natl. Acad. Sci. USA* **2011**, *108*, 5602 – 5607.
[14] S. Li, M. Hong, *J. Am. Chem. Soc.* **2011**, *133*, 1534 – 1544.
[15] M. Yamada, I. Honma, *ChemPhysChem* **2004**, *5*, 724 – 728.
[16] S. Winstein, N. J. Holness, *J. Am. Chem. Soc.* **1955**, *77*, 5562 – 5578.
[17] I. Alkorta, C. Cancedda, E. J. Cocinero, J. Z. Dávalos, P. Écija, J. Elguero, J. González, A. Lesarri, R. Ramos, F. Reviriego, C. Roussel, I. Uriarte, N. Vanthuyne, *Chem. Eur. J.* **2014**, in press.
[18] J. I. Seeman, W. A. Farone, *J. Org. Chem.* **1978**, *43*, 1854 – 1864.
[19] C. H. Gustafsson, *Finska Kemistamfundets Medd.* **1938**, *1*, 2.
[20] J. Sandström, *Acta Chem. Scand.* **1964**, *18*, 871 – 888.
[21] J. Elguero, C. Marzin, A. R. Katritzky, P. Linda, *The Tautomerism of Heterocycles*, Academic Press, New York, **1976**.
[22] I. Alkorta, J. Elguero, *J. Org. Chem.* **2002**, *67*, 1515 – 1519.
[23] I. Alkorta, F. P. Cossio, J. Elguero, N. Fresno, L. Hernandez-Folgado, S. Garcia-Granda, L. Menendez-Taboada, R. Perez-Fernandez, F. Reviriego, L. Vazquez-Vinuela, *New J. Chem.* **2013**, *37*, 2384 – 2398.
[24] V. Enchev, G. D. Neykov, *J. Mol. Struct.* **1992**, *258*, 217 – 234.
[25] V. I. Minkin, A. D. Garnovski, J. Elguero, A. R. Katritzky, O. V. Denisko, *Adv. Heterocycl. Chem.* **2000**, *76*, 157 – 233.
[26] D. A. Guthrie, A. Ho, C. G. Takahashi, A. Collins, M. Morris, J. P. Toscano, *J. Org. Chem.* **2015**, *80*, 1338 – 1348.
[27] J. Elguero, P. Goya, N. Jagerovic, A. M. S. Silva, *Italian Soc. Chem.* **2002**, *6*, 52 – 98.
[28] R. Pérez-Fernández, P. Goya, J. Elguero, *Arkivoc.* **2014**, ii, 233 – 293.
[29] J. Arriau, J. P. Campillo, J. Elguero, J. M. Pereillo, *Tetrahedron* **1974**, *30*, 1345 – 1352.
[30] O. G. Parchment, D. V. S. Green, P. J. Taylor, I. H. Hillier, *J. Am. Chem. Soc.* **1993**, *115*, 2352 – 2356.
[31] M. Cao, B. J. Teppen, D. M. Miller, J. Pranata, L. Schafer, *J. Phys. Chem.* **1994**, *98*, 11353 – 11361.
[32] F. J. Luque, J. M. López-Bes, J. Cemeli, M. Aroztegui, M. Orozco, *Theor. Chem. Acc.* **1997**, *96*, 105 – 113.
[33] G. Tschmutova, H. Ahlbrecht, *Z. Naturforsch. B* **1997**, *52b*, 535 – 542.
[34] H. Jiao, R. Nagelkerke, H. A. Kurtz, R. V. Williams, W. T. Borden, P. v. R. Schleyer, *J. Am. Chem. Soc.* **1997**, *119*, 5921 – 5929.
[35] L. Infantes, C. Foces-Foces, R. M. Claramunt, C. López, J. Elguero, *J. Mol. Struct.* **1998**, *447*, 71 – 79.
[36] C. Dardonville, J. Elguero, I. Rozas, C. Fernández-Castano, C. Foces-Foces, I. Sobrados, *New J. Chem.* **1998**, *22*, 1421 – 1430.
[37] G. I. Yranzo, E. L. Moyano, I. Rozas, C. Dardonville, J. Elguero, *J. Chem. Soc. Perkin Trans. 2* **1999**, 211 – 216.
[38] J. B. Alderete, J. Belmar, M. Parra, C. Zúñiga, *Bol. Soc. Chil. Quim.* **2000**, *45*, 85 – 89.
[39] G. A. Chmutova, O. N. Kataeva, H. Ahlbrecht, A. R. Kurbangalieva, A. I. Movchan, A. T. H. Lenstra, H. J. Geise, I. A. Litvinov, *J. Mol. Struct.* **2001**, *570*, 215 – 223.
[40] E. Kleinpeter, A. Koch, *J. Phys. Org. Chem.* **2001**, *14*, 566 – 576.
[41] W. Holzer, K. Hahn, T. Brehmer, R. M. Claramunt, M. Pérez-Torralba, *Eur. J. Org. Chem.* **2003**, *2003*, 1209 – 1219.
[42] H. Lin, D.-l. Wu, L. Liu, D.-z. Jia, *J. Mol. Struct.* **2008**, *850*, 32 – 37.
[43] V. Enchev, S. Angelova, *J. Mol. Struct.* **2009**, *897*, 55 – 60.
[44] G. A. Chmutova, E. R. Ismagilova, T. I. Madzhidov, *Russ. J. Gen. Chem.* **2009**, *79*, 1919 – 1928.
[45] I. Soteras, M. Orozco, F. J. Luque, *J. Comput. Aided Mol. Des.* **2010**, *24*, 281 – 291.
[46] N. A. Abood, R. A. Al-Shlhai, *J. Chem. Pharm. Res.* **2012**, *4*, 1772 – 1781.
[47] A. Amar, H. Meghezzi, A. Boucekkine, A. Saidoun, Y. Rachedi, M. Hamdi, *Int. J. Pharm. Chem. Biol. Sci.* **2013**, *3*, 745 – 751.
[48] D. Tarabová, S. Soralová, M. Breza, M. Fronc, W. Holzer, V. Milata, *Beilstein J. Org. Chem.* **2014**, *10*, 752 – 760.
[49] J. Elguero, A. R. Katritzky, O. V. Denisko, *Adv. Heterocycl. Chem.* **2000**, *76*, 1 – 84.
[50] P. J. Taylor in *The Scope and Limitations of LSER in the Study of Tautomer Ratio, Vol. 76* (Ed. L. Antonov), Wiley-VCH, Weinheim, **2014**, pp. 277 – 304.
[51] A. D. Becke, *J. Chem. Phys.* **1993**, *98*, 5648 – 5652.
[52] C. T. Lee, W. T. Yang, R. G. Parr, *Phys. Rev. B* **1988**, *37*, 785 – 789.
[53] M. J. Frisch, J. A. Pople, J. S. Binkley, *J. Chem. Phys.* **1984**, *80*, 3265 – 3269.
[54] Gaussian 09 (Revision D.01)M. J. Frisch, G. W. Trucks, H. B. Schlegel, G. E. Scuseria, M. A. Robb, J. R. Cheeseman, G. Scalmani, V. Barone, B. Mennucci, G. A. Petersson, H. Nakatsuji, M. Caricato, X. Li, H. P. Hratchian, A. F. Izmaylov, J. Bloino, G. Zheng, J. L. Sonnenberg, M. Hada, M. Ehara, K. Toyota, R. Fukuda, J. Hasegawa, M. Ishida, T. Nakajima, Y. Honda, O. Kitao, H. Nakai, T. Vreven, J. Montgomery, J. A., J. E. Peralta, F. Ogliaro, M. Bearpark, J. J. Heyd, E. Brothers, K. N. Kudin, V. N. Staroverov, R. Kobayashi, J. Normand, K. Raghavachari, A. Rendell, J. C. Burant, S. S. Iyengar, J. Tomasi, M. Cossi, N. Rega, N. J. Millam, M. Klene, J. E. Knox, J. B. Cross, V. Bakken, C. Adamo, J. Jaramillo, R. Gomperts, R. E. Stratmann, O. Yazyev, A. J. Austin, R. Cammi, C. Pomelli, J. W. Ochterski, R. L. Martin, K. Morokuma, V. G. Zakrzewski, G. A. Voth, P. Salvador, J. J. Dannenberg, S. Dapprich, A. D. Daniels, Ö. Farkas, J. B. Foresman, J. V. Ortiz, J. Cioslowski, D. J. Fox, Gaussian, Inc., Wallingford, **2009**.
[55] D. E. Woon, T. H. Dunning, *J. Chem. Phys.* **1995**, *103*, 4572 – 4585.
[56] T. H. Dunning, *J. Chem. Phys.* **1989**, *90*, 1007 – 1023.
[57] A. G. Baboul, L. A. Curtiss, P. C. Redfern, K. Raghavachari, *J. Chem. Phys.* **1999**, *110*, 7650 – 7657.
[58] J. Tomasi, B. Mennucci, R. Cammi, *Chem. Rev.* **2005**, *105*, 2999 – 3094.
[59] R. F. W. Bader, *Atoms in Molecules: A Quantum Theory*, Clarendon Press, Oxford, **1990**.
[60] T. A. Keith in AIMAll, TK Gristmill Software (aim.tkgristmill.com), **2011**, TK Gristmill Software (aim.tkgristmill.com).
[61] J. Catalan, J. L. G. Paz, M. Sánchez-Cabezudo, J. Elguero, *Bull. Soc. Chim. Fr.* **1986**, *3*, 429 – 435.
[62] V. Barone, C. Adamo, *J. Phys. Chem.* **1995**, *99*, 15062 – 15068.
[63] L. Gorb, J. Leszczynski, *J. Am. Chem. Soc.* **1998**, *120*, 5024 – 5032.
[64] I. Alkorta, J. Elguero, *J. Chem. Soc. Perkin Trans. 2* **1998**, 2497 – 2504.
[65] I. Alkorta, I. Rozas, J. Elguero, *J. Chem. Soc. Perkin Trans. 2* **1998**, 2671 – 2676.
[66] B. Balta, V. Aviyente, *J. Comput. Chem.* **2004**, *25*, 690 – 703.
[67] V. Enchev, M. Markova, S. Angelova, *Chem. Phys. Res. J.* **2007**, *1*, 1 – 36.
[68] N. Markova, L. Pejov, V. Enchev, *Int. J. Quantum Chem.* **2015**, *115*, 477 – 485.
[69] J. A. Platts, *Phys. Chem. Chem. Phys.* **2000**, *2*, 973 – 980.
[70] J. A. Platts, *Phys. Chem. Chem. Phys.* **2000**, *2*, 3115 – 3120.

Received: April 15, 2015
Published online on ■■ ■■, 2015

ARTICLES

C. Trujillo, G. Sánchez-Sanz, I. Alkorta, J. Elguero*

■■ – ■■

Computational Study of Proton Transfer in Tautomers of 3- and 5-Hydroxypyrazole Assisted by Water

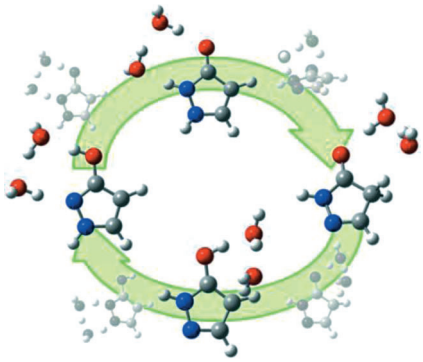

Just add water: A theoretical study of the tautomerism of 3- and 5-hydroxypyrazole focusing on the solvent effects as well as on proton transfer assisted by one and two water molecules is reported. A significant reduction of the transition barriers upon solvation is found. In addition, the tautomerism processes of ionic species (both anions and cations) isolated and assisted by one water molecule are studied.